Sigma J Eng Nat Sci, Vol. 40, No. 2, pp. 252–267, June, 2022

Sigma Journal of Engineering and Natural Sciences
Web page info: https://sigma.yildiz.edu.tr
DOI: 10.14744/sigma.2022.00030

Research Article

The hydrogeological functioning of the karstic aquifer in Sidi Kada Mountains (North-Western Algeria) from hydrochemical records

Benyekhlef BENAMINA[1], Habib AZZAZ[1], Benali BENZATER[2], Abderrahmane HAMIMED[2,*]

[1]Science and Technology of Water Laboratory, University of Mascara, Algeria
[2]Biological Systems and Geomatics Laboratory, University of Mascara, Algeria

ARTICLE INFO

Article history
Received: 09 September 2020
Accepted: 28 June 2021

Key words:
Hydrogeology; Hydrochemistry; Karst Aquifers; Sidi Kada Mountains; North-western Algeria

ABSTRACT

This study focuses on the hydrodynamic and hydrochemical functioning of the karst system in Sidi Kada Mountains. These later extend between the Ghriss plain in the North and the Saida Mountains in the South. The hydrochemical approach was used to understand the hydrodynamic behaviour of the karst system which is represented by dolomitic limestone formation of Upper Jurassic. The geological data were used to delimit an impluvium with an area of 535.1 km^2 and a perimeter of 220.7 km. The functioning of this karst system was studied using several physic-chemical parameters, namely pH, temperature, electrical conductivity, TDS, Ca^{2+}, Mg^{2+}, Na^{+}, HCO_3^-, Cl^-, NO_3^-, SO_4^{2-}. Frequency distributions of the water electrical conductivity (CFD) indicate that the system is characterized by two hydrodynamic sub-regimes, in which fracture networks control the base flow and conduit networks control the quick flow. The results of the hydrochemical analysis show that the waters facies are bicarbonated and magnesian. During periods of high water, the contents of chemical elements decreased, except for calcium and nitrates. During periods of low water, the participation of the saturated zone generates an increase in Mg^{2+} contents. The waters are typically characterised by an average conductivity of 848 µS/cm in deep waters. The shallow waters, influenced by anthropogenic actions, have an average conductivity of 1344 µS/cm and waters where exists the evaporite lenticular mass have relatively high values of conductivity, ranging from 1886 to 2644 µS/cm with an average of 2102 µS/cm. The good correlation between the chlorides and sulphates indicates the leaching of the soil layer. The correlation between Ca^{2+} and SO_4^{2-} is negative but weak (r = −0.176), implied that Ca^{2+} was no derived from gypsum in the majority of samples. In contrast the water points whose chemistry is marked by the dissolution of gypsum or anhydrites have a good correlation between Ca^{2+} and SO_4^{2-} (r = 0.93). The supersaturating regarding calcite and dolomite indices indicates mainly a flow in the saturated zone and through the unsaturated zone with a relatively high pCO_2 (from 1.5×10^{-2} to 4×10^{-2}). Biogenic CO_2 initiates the mineralisation process in the unsaturated zone within an open system. The relationship between the saturation indices regarding calcite and dolomite shows that 87% of water varied from equilibrium and oversaturated. This is indicative of a slightly aggressive water with relatively slow circulation.

***Corresponding author.**
*E-mail address: hamimed@univ-mascara.dz

This paper was recommended for publication in revised form by Regional Editor Pouria Ahmadi

Published by Yıldız Technical University Press, İstanbul, Turkey

Cite this article as: Benamina B, Azzaz H, Benzater B, Hamimed A. The hydrogeological functioning of the karstic aquifer in Sidi Kada Mountains (North-Western Algeria) from hydrochemical records. Sigma J Eng Nat Sci 2022;40(2):252–267.

INTRODUCTION

The karst fascinates amateurs and professionals with the diversity of its forms which start on the surface and extend to depths, still untouched by any exploration. Many scientific communities are still trying to unlock its secrets and offer keys to explain the past and present functioning of a karst system. In addition to its remarkable morphological expressions, its drinking water resources make it a very important topic, especially in the Mediterranean region where this type of aquifer is prevailingand the drinking water needs are significant [1,2].

These aquifers are distinguished from the porous aquifers by the high degree of heterogeneity featured in both surface and underground [3]. Carbonate sedimentary formations such as limestone and dolomite are the most important karst-prone rocks [4]. However, karstification can also occurs in other rock types such as carbonatic conglomerates [5], carbonatic metamorphic rocks such as marble or calcite [6], and evaporitic formations such as gypsum or anhydrite [7].

Because of their hydrogeological characteristics, karst aquifers are particularly vulnerable to anthropogenic activities and are difficult to manage [8-10]. Many researchers carried out hydrogeochemical analyses to assess the geological and anthropogenic influences on the hydrochemistry of aquifers [11–18]. These analyses have been successfully used to reveal groundwater circulation depth, vulnerability and hydrogeochemical evolution [19-21]. Groundwater flows in karst aquifers are extremely variable in space and time, and depend on several factors such as the hydrogeological heterogeneity of the system, the configuration of the karst network and local recharge conditions [22]. Understanding the functioning of the karst aquifer system is generally an essential condition to improve the management of water resources, their protection and their vulnerability study [23]. Studies of karst systems have traditionally focused on the analysis of natural responses of sources to recharge events. Also, hydrogeological research for this type of aquifer can be achieved by studying techniques based on natural hydrodynamic responses [24–26]. However, the high degree of anisotropy of this type of aquifer requires the application of different categories of approaches: hydrogeological, geomorphological, geophysical, structural, etc. Several factors, such as climate, geology and geomorphology can change the dynamics of groundwater. Although hydroclimatic conditions remain the main factors responsible for the evolution of the functioning of karst aquifers [27–29], the chemical composition of groundwater depends on the crossed rocks nature, the residence time of water in the system, the climatic conditions prevailing in each zone and geochemical processes along the groundwater flow paths [30–34, 23]. The hydrochemical data were analyzed using different procedures. The electrical conductivity frequency distributions (CFD) of the spring water inform on the variability of the mineralization and on the degree of functional karstification into the system [30, 35]. Unimodal distributions are indicative of little annual variation in mineralization and consequently hydrochemical homogenization, mostly due to a low degree of karstification (diffuse flow), while multimodal distributions should be associated with systems having higher degree of karstification (conduit flow system) [35]. A methodology for a better quantification and interpretation of the conductivity frequency distributions (CFD) has been published by Massei et al. (2007) [36]. After this approach, a single water type transported through a karst conduit network is chemically homogeneous and its electrical conductivity shows a normal distribution. The analysis of CFD allows the identification of different modes, corresponding to water types influenced by hydrological and meteorological conditions (recharge, recession and depletion), and their contribution to the spring flow. The contribution of each peak to the CFD can be quantitatively assessed, which can be useful to characterize the aquifer behaviour and mixing processes [35].

The Piper diagram constitutes a basic tool for spatial characterization of the chemical composition of waters. It allows establishing clusters or families depending on lithological, geographical and anthropogenic factors [37–39]. Binary diagrams have also been broadly used to interpret hydrochemical data. The relationship between different chemical components dissolved in water can be useful to identify and to characterize hydrogeochemical processes in karst systems [40, 41]. The use of natural hydrochemical tracers such as dissolved organic carbon (DOC), nitrates (NO_3^-), chlorides (Cl^-), or magnesium (Mg^{2+}) is useful for characterizing infiltration processes, water transit times, flow conditions and, above all, the degree of participation of saturated and unsaturated zones in the functioning of karst systems [27, 40, 44–47]

To better understand the role of the unsaturated zone in the acquisition of groundwater chemistry, calcocarbon balances are particularly used. The equilibrium pCO_2 and the saturation index with respect to calcite and dolomite are the well suited elements for understanding the hydrodynamic functioning of karst aquifers. They provide valuable information on the origin of the different types of water flowing

at the outlet, on their flow conditions and their residence times [35].

The Sidi Kada Mountains (located in Northwest Algeria) is a semi arid area, represented by a calcareous-dolomitic plateau of Kimmeridgian (Upper Jurassic) age. Because of the lack of surface-water and precipitation, groundwater has been the main water resource in this area. Sustainable management of groundwater has become a critical issue for this area. Understanding the hydrochemical characteristics of the local groundwater could provide guidance for sustainable groundwater development.

This research mainly presents a hydrochemical investigation of groundwater in Sidi Kada Mountains to determine the hydrochemical characteristics, mineral sources, and hydrochemical evolution along the groundwater flow path. The absence of speleological networks and caves in our study area gives the impression that the flows are mainly in the volumes of fissured rock with low permeability. Epikarst plays an important role in regulating aquifer recharge: part of the water infiltrated into the epikarst is stored in its base and flows slowly through the underlying cracked volumes (base flow); if the infiltration is sufficient, part of the water directly overflows from the epikarst to the karst network (rapid flow). The springs are characterized by a relatively low and constant spring flows. Its hydrochemical characteristics are mainly determined by the geochemical process of rocks in the area (dolomitic limestones), and are affected by climate, precipitation, soil, vegetation and human activities. The precipitation in this area is the main recharge of groundwater.

The main objective of this study is to characterize the hydrogeological functioning of the karst system in Sidi Kada Mountains (Figure 1), based on its hydrodynamic properties and its hydrochemical response during the sampling period, with rainfall variability, and therefore different hydraulic conditions. To do so, the first objective is to characterize water types and origins over the hydrogeological catchment using natural hydrochemical tracers.

STUDY AREA

The Sidi Kada Mountains cover an area of 486.1 km2, located in the North-West of Algeria between longitudes 0° 12' E and 0° 36' E and latitudes 35° 13' N and 35° 22' N (Figure 1), and aligned with the Beni-Chougrane Mountains, which is the main massif between the Mediterranean and the High Oran Plains. This Mountain barrier is located between 540 m and 1200 m above the sea level [48].

The region is characterized by a semi-arid climate, with a mild winter and a hot summer in addition to relatively remarkable of rainfall seasonal variations. The average yearly precipitation value during the period 1969–2016 is about 473mm with relative monthly irregularities (69 mm

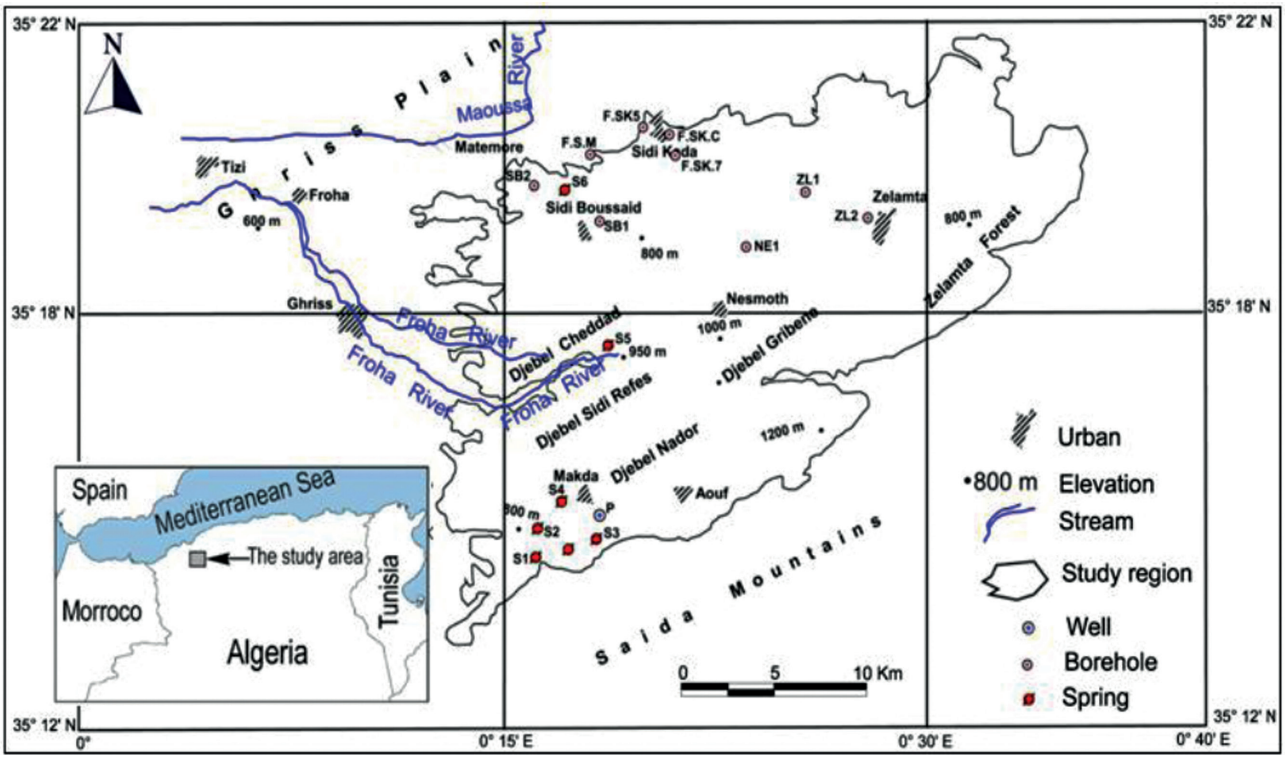

Figure 1. Location of the study area map.

for December and 3 mm for July). The Sidi Kada Mountains are drained superficially by the Froha wadi. The mean annual relative humidity of the air is about 65% and the mean annual temperature is of 25°C. These climatic conditions are favorable for the weathering of rocks and consequently have a significant impact on the groundwater quality.

GEOLOGY

The Sidi Kada Mountains are spread between the Saida Mountains in the South and the Ghriss plain in the North. The Tiffrit's granite mole locally separates Sidi Kada and Saida Mountains (Figure 2). The structural of the study area is characterized by horsts and grabens. These reliefs show a brittle tectonics with faults oriented Northwest-Southeast and northeast-southwest.

Through Sidi Kada Mountains, the Kimmeridgian dolomitic limestones with a passage in lenticular mass or fibrous gypsum, clays and marls, overcome (surmounts) the Lusitanian Marls and sandstones-dolomitic alternations. Locally, the Kimmeridgian is surmounted by Quaternary formed by clay-sand with gravel alluvial deposits occupying the grabens zones. The tectonic of the region generated

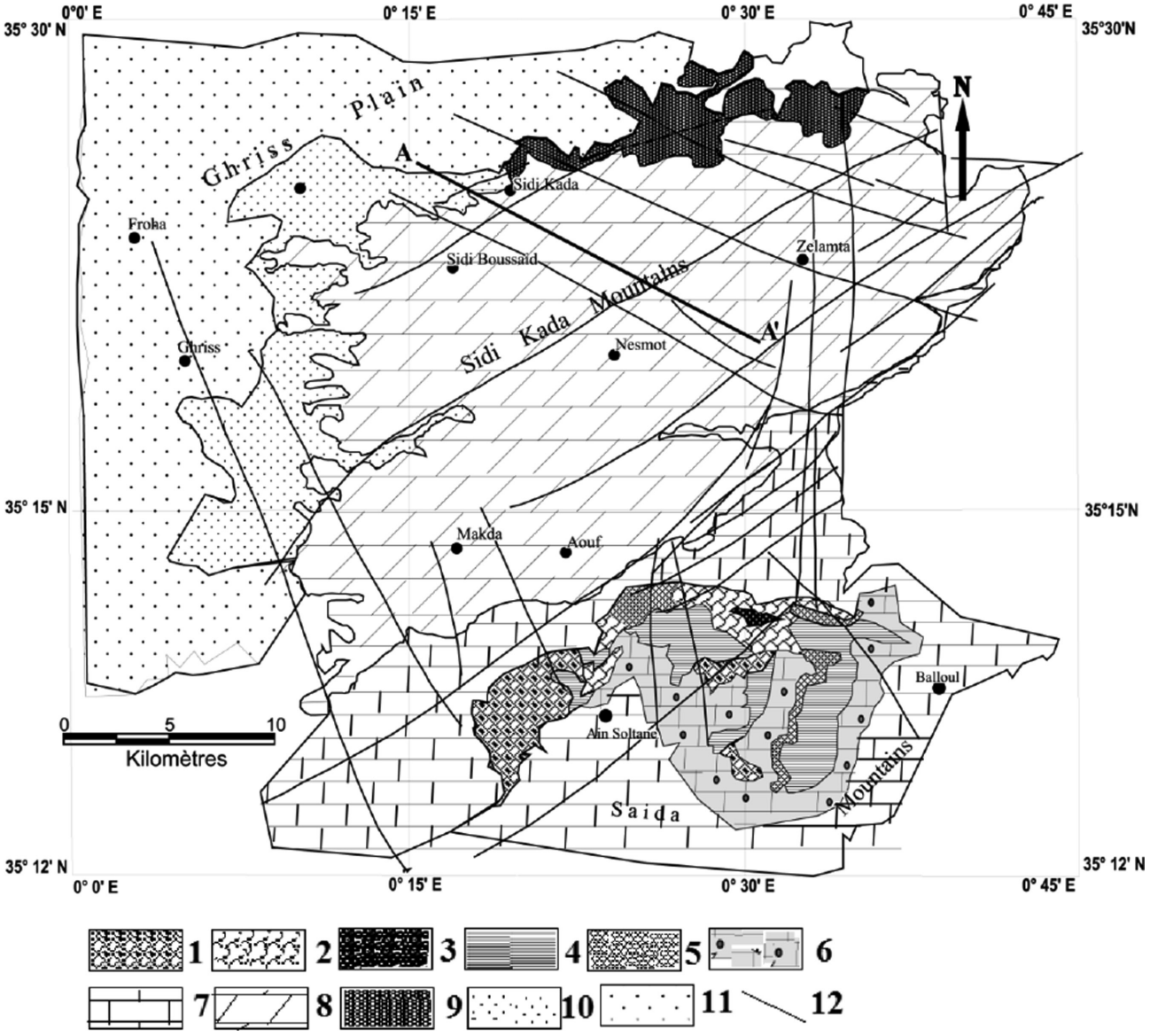

Figure 2. Geologic map. 1- Paleozoic, 2- Devonian, 3- Carboniferous, 4- Permo-Triassic, 5- Triassic, 6- Middle Jurassic (Dogger), 7- Upper Jurassic (Oxfordien), 8- Upper Jurassic (Kimmeridjien), 9- Miocene, 10- Plio-queternary, 11- Quaternary, 12- Fault. (Ref: geological Mostaganem and Saida map 1/200000; National Agency of Water Resources).

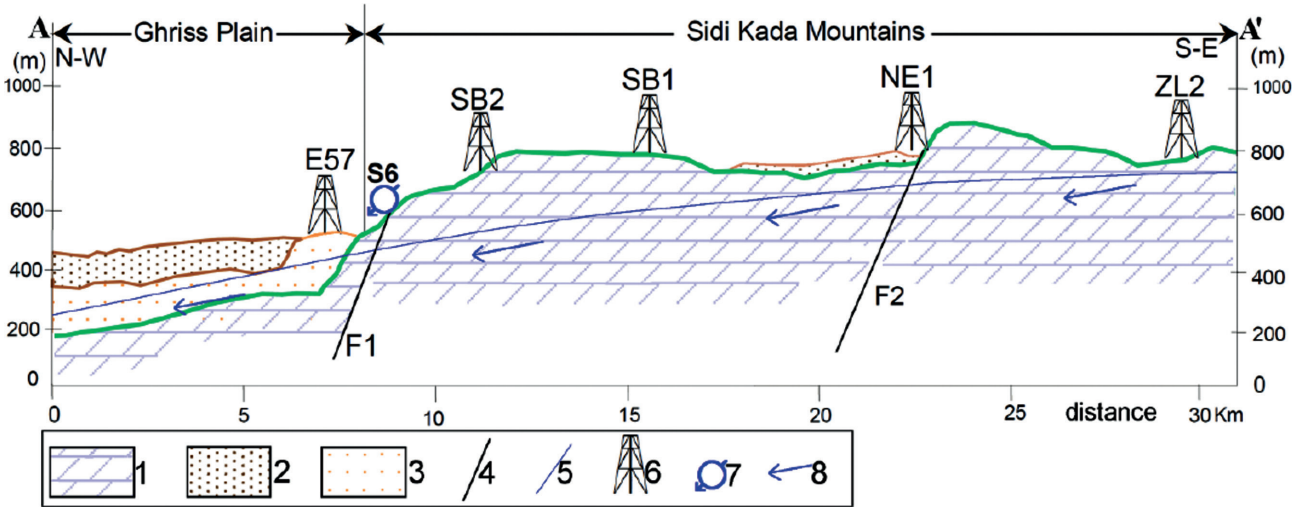

Figure 3. Cross section: A-A' (1- Upper Jurassic (Kimmeridjien); 2- Quaernary; 3- Plio-quaernary; 4- Fault; 5- Water level; 6- Borehole; 7- Overflow spring; 8- Water flow direction. (Ref: borehole's cross - Water Resources Direction).

graben with releases that vary between 10 to 50 m (Figures 2 and 3).

HYDROGEOLOGY

The Kimmeridgian dolomitic limestones represent the main aquifer with an average thickness of 250 m outcrop over more than 90% of Sidi Kada Mountains with a plunge to the North under the Plio-Quaternary alluvium. The aquifer bottom is represented by the alternations of marl, sandstone and dolomites of the Lusitanian (Figure 3).

The piezometric map shows a general flow oriented South-East North-West with depths varying between 8 and 101m. This aquifer is recharged from the outcrop areas. The discharge rates of the existing boreholes in the North of the study area oscillate between 10 l/s (F.SKC borehole, see Figure 1) to 20 l/s (F.SK5 borehole, see Figure 1).The boreholes in the southern part of the study area vary between 7 l/s (NE borehole) to 15 l/s (ZL1 borehole), whereas in the springs, the flow rates vary between 0.60 l/s and 2.1 l/s (1.2 l/s for the spring S1 (1.10 l/s high water and 0.80 l/s low water), 0.95 l/s for the spring S4 (1.50 l/s for high water and 0.60 l/s for the low water) and 1.90 l/s for the spring S6 (2.1 l/s high water and 1.80 l/s low water). the piezometric level in the well (P) is 916 m in the high water period and 913 m in the low water period.

METHODOLOGY AND TECHNIQUE

The hydrochemical study of the dolomitic limestone aquifer water was carried out on the basis of seasonal monitoring over the period 2013-2018 through 16 representative water points (seven sources, eight boreholes and one well) (Figure 1).

The pH, temperature, conductivity, salinity, dissolved oxygen and TDS were measured in-situ using a multi-parameter device, model HI 9828.

The water chemical analysis, namely the cations (Ca^{2+} Mg^{2+}, Na^{+}, K^{+}) and the anions (HCO_3^-, Cl^-, SO_4^{2-}, SiO_2, NO_3^-) were carried out at the National Agency of water resources (ANRH) of Oran and the Water Distribution Agency (ADE) laboratories.

The processing of hydrochemical data using the Diagram software [49] allowed us to study the binary relationships between the chemical elements (chlorides, sulphates, sodium, saturation index and CO_2 pressure). The frequency distributions of electrical conductivity (CFD) inform us about the variability of the mineralisation and chemical composition of the water [30].

RESULTS AND DISCUSSION

The results of water analysis as shown in Table 1 allow characterizing the water in the region according to their conductivity values. The boreholes water located at the foothills of Sidi Kada Mountains in the northern part of the basin and the springs located in the south-west are characterized by conductivity values ranging from 774 to 1100 µS/cm. For the springs in the north part of the basin and the boreholes located in the south-eastern, those values vary between 1200 and 1402 µS/cm. However, the springs located in the center of the study area are individualized by the high values of conductivity ranging from 1886 to 2644 µS/cm. The boreholes located in the south-Est (Zelamta and Nesmot regions) show relatively high hydrochemical contents compared to the boreholes located in the northern foothills. This is due to the influence of the Lusitanian aquifers (sandstone, dolomite and marl) which does not

Table1. Presentation of the physicochemical parameters of Sidi Kada Mountains aquifer.

Sample		TDS	T°C	pH	c25°C	Ca [mg/l]	Mg [mg/l]	Na [mg/l]	HCO3 [mg/l]	Cl [mg/l]	SO4 [mg/l]	NO3 [mg/l]	Mg/Ca	IsC	IsD	pCO_2
Group 1	Min	378	16.76	7.20	756	31	8	23	460	41	19	5	0.09	0.15	–0.32	0.0124
	Average	404	21.72	7.36	848	79.5	47	25	477	46	25.1	17.7	1.24	0.38	0.22	0.0181
	Max	419	25.83	7.50	1107	154	80	28	514	54	32	25	4.26	0.58	0.68	0.0289
Group 2	Min	973	14.85	7.16	1249	61	30	51	365	101	113	80	0.25	–0.25	–0.24	0.0082
	Average	1030	17.60	7.30	1344	105	77.6	58.6	401.7	131.7	130.8	93.8	1.37	0.26	0.10	0.0168
	Max	1133	20.10	7.61	1429	196	105	64	417	157	176	120	2.84	0.66	0.62	0.0237
Group 3	Min	897	14.44	7.13	1886	44	86	177	556	184	320	10	0.82	–0.16	–0.21	0.0324
	Average	1025	14.85	7.14	2102	99	111	223	589.8	205.2	439	10.7	2.04	0.11	–0.04	0.0335
	Max	1321	16.07	7.17	2644	174	136	357	642	249	786	15	4.87	0.36	0.27	0.0350

outcrop. The pH values of the study area ranged from 7.13 to 7.84.This means that the waters in this area are neutral and correspond to waters of the carbonate system [50]. The temperature varies between 14.95°C and 23.74°C and the salinity is in the range of 0.36 and 1.39 g/l. The total dissolved solids (TDS) is divided into three ranges: the first varies from 331 to 552 mg/l, corresponding to the boreholes located in the north and springs located in the south-west, the second is in the range 630-888 mg/l which correspond to the perched emergency (shallow groundwater) located in the high altitudes, and the third ranged from 990 to 1730 mg/l, corresponding to the sources located in the center of the basin (water points whose chemistry is marked by gypsum or anhydrite). The waters of the first range are fresh waters according to the international standard with TDS < 600 mg/l.

The decomposition of the conductivity frequency distributions (CFD) into different peaks, following the approach proposed by Massei et al. (2007) [36], can be useful for the identification of different sources of water and the influence of hydrologic (recharge, recession and depletion) and meteorological conditions on their contribution to springs flow.

This approach has been applied at monthly scale and at each rain event. The EC data set is recorded during the period Junary 2014-March 2015 at S1, S4, S5 and S6 springs (Figure 1). These four springs present diverse patterns of hydrogeological behaviours, with differing hydrochemical responses to recharge events (Figure 4).

Thus, the CFD values for the EC data corresponding to S1 spring have been divided in three different peaks or modes (P1, P2 and P3), representing water types with different mineralization, which contributed to the spring flow during the research period (Figure 4). The P1 (20%) represented the first precipitation after the dry period (recharge). The high water period is represented in P2. These waters are drained with a progressively longer residence time due to either slow infiltration or storage in the saturated zone. Groundwater runoff components released from small and medium karst fissures. The pick 3 (P3) with a higher conductivity should represent the drainage of fissures and matrix (mainly saturated zone) during depletion period.

In contrast, S4 Spring (Figure 4), the peak P1 represents a dilution of the spring water after dry period (rainfall event of 49 mm in June 2014). These can be represented a rapid infiltration of low conductivity surface water through fractures, which then directly drained to the spring through conduits (water dilution). The largest peak (P2) corresponds to periods when the aquifer is either slowly filling or draining and as such reflects a "baseline" specific conductance. The P3 corresponds to the waters bases period with absence of rainfall grades. These waters are drained through the fissures (saturated zone) during depletion period. The peak P4 reflect the progressive increment of water mineralization in the spring, caused by corresponding changes in SO_4^{2-}, Cl^-, Mg^{2+} and Ca^{2+} contents, produced as consequence of recharge events that provoke a piston effect (event rainfall 54 mm in March 2014). This increase is linked to the contribution of evaporites (gypsum or anhydrite).

For the S5, the CFD values measured in the water from spring (Figure 4) show relatively high variability. The P1 reflects the progressive increment of water mineralization in the spring, after dry period (June 2014 and September 2014), caused by corresponding changes in Mg^{2+} and Ca^{2+} contents, and produced as consequence of recharge events. This corresponds to the water previously stored within the unsaturated zone towards the spring (event rainfall 49 mm and 53 mm respectively). These increments are proportional to the quantity and magnitude of rainfalls recorded during recharge events, with a relatively fast response time. The P2 peak contributes 67% to the global frequency distribution and represents the water drained during the high water period (presence of rain), with a low conductivity variation. Peaks P3 (26%) should represent the drainage of fissures and matrix (mainly saturated zone) during depletion period. After the event rainfall (54 mm in March 2014), the piston effect causes variations in hydrochemical

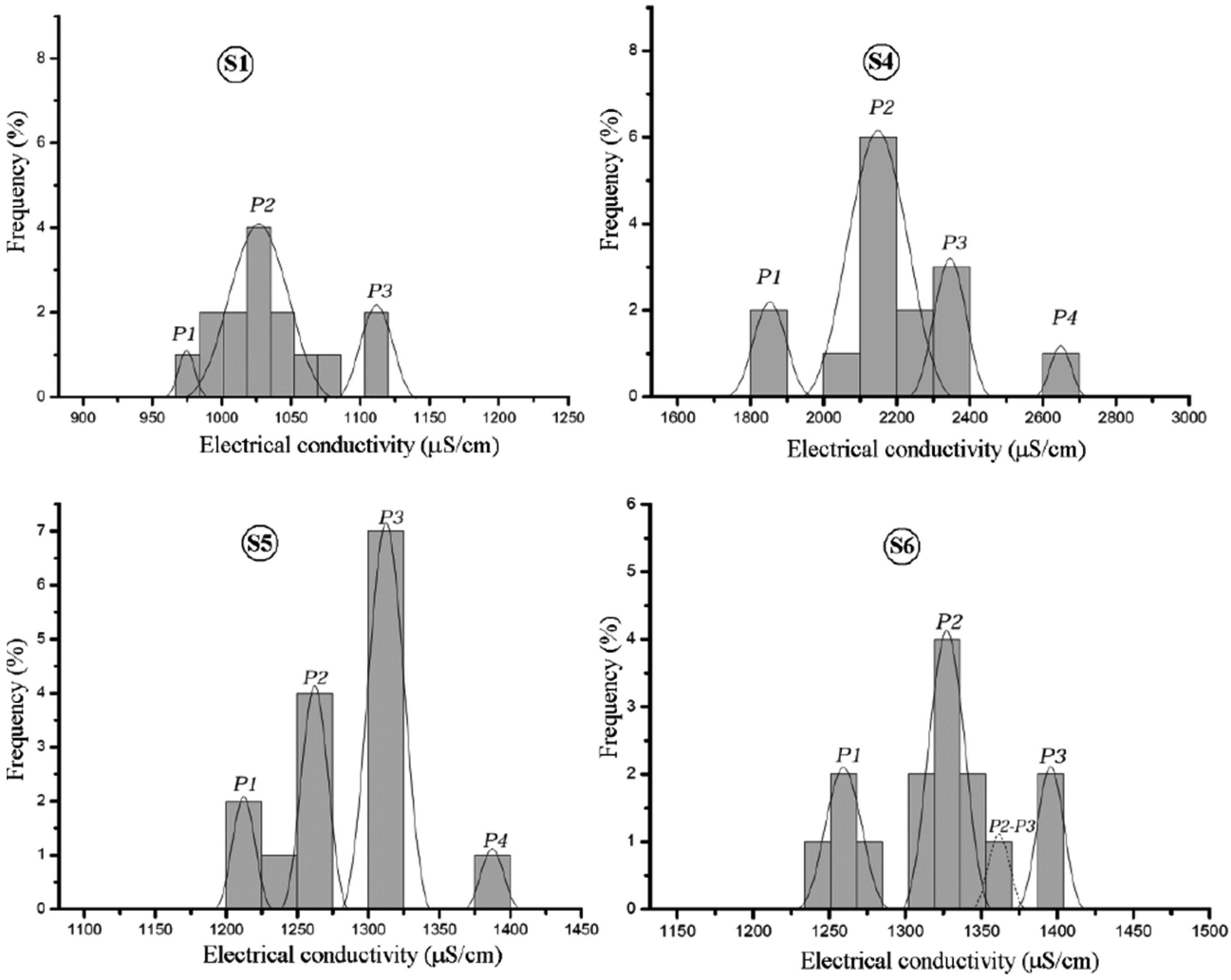

Figure 4. The electrical conductivity frequency distributions (CFD) for the springs S1, S4, S5 and S6.

components, characterized by an increase of Mg^{2+}/Ca^{2+} ratio, which indicate the participation of the water previously stored in unsaturated zone (P4) [46, 35]. The P1, P2 and P4 (74%) represent the water drained from the unsaturated zone.

Finally, the CFD obtained from the EC data of S6 spring presents three major modes (Figure 4). The Peak P1 (40 % of the total distribution) corresponds to the water with the lowest EC values (high water condition), rapidly flowing from the soil and epikarst to the spring through karst conduits. These waters types related at events rainfall (54 mm in March 2014; 49 mm in June 2014 and 53 mm in September 2014). The peak P2 represents the transition between the previous hydrodynamic conditions, during which karst conduits with different hydraulic conductivities are still active and they interact with the low permeable or matrix portion of the aquifer. The last Peaks P3 (20 %) should represent the drainage of fissures and matrix (mainly saturated zone) during depletion period. Peak $P_{2\text{-}3}$ corresponds to periods when the aquifer is draining. The hydrogeological functioning of the S4, S5 and S6 springs are fundamentally influenced by the unsaturated zone of the aquifer (peaks P1 and P2 for S6 and P1, P2 and P4 for S4and S5), which affect their functioning more than does the saturated zone (P3) (especially under recharge conditions). These springs drain an aquifer with a moderate degree of development of karst drainage, which means that the hydrodynamic and hydrochemical responses present some inertia as regards precipitation events. In contrast, the CFD values measured in the water from S1 (Figures 4 and 6b) show a low variability in conductivity (40 µS/cm). The hydrogeological functioning of the S1 is fundamentally influenced by the saturated zone of the aquifer. Both zones (saturated and unsaturated zone) present a relatively low degree of functional karstification. The springs are characterized by two hydrodynamic subregimes, in which fracture networks control the base flow

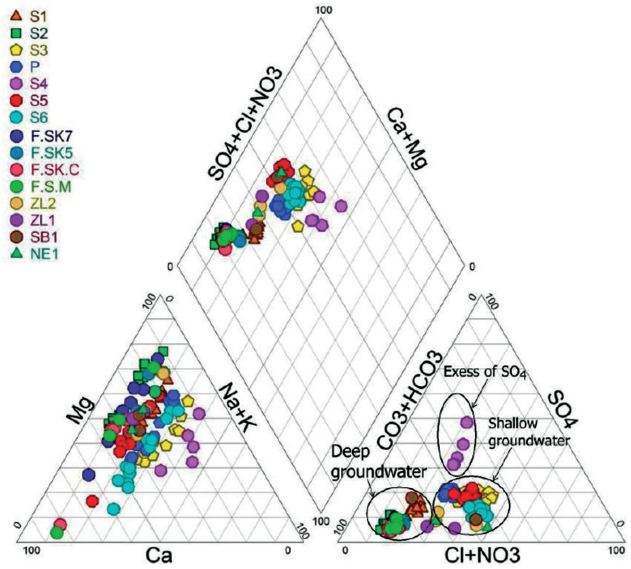

Figure 5. Piper diagram: presentation of the geochemical facies of the groundwater of Sidi Kada Mountains. (S1, S2, S3, S5, S5 and S6 are the springs, P is well, and F.SK, F.SK5, F.SK.5, F.S.M, ZL2, ZL1, SB1 and NE1 are the boreholes).

and conduit networks control the quick flow, as mentioned by [22].

For most cases, the SO_4^{2-} contents vary from 19 to 176 mg/l, while some samples are characterized by high contents of SO_4^{2-}, varying between 320 and 786 mg/l (Table 1). This may be due to a layer of gypsum and/or anhydrite ($CaSO_4+H_2O$ or $CaSO_4$) near their measurement locations as mentioned by [51–53] and existence of gypsum lenses. Generally, NO_3^- concentrations vary between 15 to 25 mg/l with the except for water points located near urban agglomerations which show high contents (80 to 120 mg/l).

The presentation of the water analysis results on the Piper diagram (Figure 5) shows that the waters of the study area are divided into two chemical facies: 59% of waters are bicarbonate calcium and magnesium and 41% are chlorinated and sulphated magnesium and calcium. The waters with high concentrations of chlorides and sulphates are from epikarst, influenced by human actions (agriculture and domestic wastewater discharge) or by the existence of evaporite.

The variograms presented in Figure 6 show good correlation between the major chemical elements (HCO_3^-, Mg^{2+}, SO_4^{2-}, Cl^- and Na^+) and the conductivity. The decrease of the electrical conductivity (EC) after each rain indicates the dilution effect [10] (Figure 6). The shallow karst zones expedite the transport of recharge, so shallow systems respond very quickly to rain events, always exhibiting rapid increases in EC (Figure 6a). A slight increase of the EC after rain event means a mixture between the waters of the saturated zone and the unsaturated zone [47,54, 55] (Figure 6).

The synchronous increase in precipitation and conductivity indicates the arrival of water with a long residence time on emergence by the piston effect. During recharge events in shallow waters, the first flood event leads to an increase of the ratios Mg^{2+}/Ca^{2+}: 1.25 on 07/03/2014 and 1.00 on 03/03/2014, and 3.00 on 05/06/2014 and 2.00 on 02/06/2014. Similar results are found in the deep water showing an increase of the ratios Mg^{2+}/Ca^{2+}: 4.4 on 27/03/2014 and 1.4 on 03/03/2014, and 3.5 on 01/06/2014 and 2.5 on 14/06/2014. The increase in the ratios Mg^{2+}/Ca^{2+} results in the mobilization the water storage in the unsaturated zone of the aquifer. For comparison, the shallow water and the deep water have residence time of 15 days and 45 days, respectively.

The variations in Ca^{2+} and Mg^{2+} concentrations are in the ranges 30–196 and 32–136 mg/l, respectively. The summer floods at the surface water cause a relatively rapid increase in Ca^{2+} concentrations (about 15 days) with a decrease in Mg^{2+} elements (Figure 6a) confirmed by significant negative correlation (r = –0.944) (Figures 7a and b). This indicates that the water is drained from the unsaturated zone, whereas the waters drained from the saturated zone show a relatively slow residence time (about 45 days) (Figure 6b).The deep waters are characterized by a ratio Mg^{2+}/Ca^{2+} greater than 1.2 throughout the year (1.24 to 4.25) (Figure 6b). This indicates a large predominance of dolomite which confirms the geological data [21, 47, 50, 51, 56]. While for the shallow water, the ratio is ranged between 0.5 and 3.5 (Figure 6a). The NO_3^- leaching can occur throughout the year (Figure 6a), with particularly peaks concentrations during fall infiltration and summer flooding [57–59] (Figure 6a). In the shallow water during recharge events, the first flood event leads to an increase of NO_3^- concentrations: 121 mg/l on 05/06/2014 and 112 mg/1 on 15/ 05/2014, and 144 mg/l on 27/09/2014 and 104 mg/l on 31/08/2014, associated with increase of Mg^{2+}/Ca^{2+}. The increase in concentrations results in the mobilization of NO_3^- storage in soil and the unsaturated zone of the aquifer during low-water periods (Figure 6a). However, in the deep waters (Figure 6b), there is an increase of NO_3^-: 23 mg/l on 15/05/2014 and 18 mg/l on 15/ 05/2014, with an increasing of Mg^{2+}/Ca^{2+}.

The chlorides fluctuate with nitrates, recording a significant positive correlation (r = 0.78) (Figure 7a). This correlation suggests an anthropogenic input indicating the same origin (soil and epikarst) of these elements which are considered as tracers of infiltration [54, 60]. There are significant correlation between SO_4^{2-} and Cl^- (r = 0.97) indicating an anthropogenic origin (Figure 7a). Whereas, in S4 the significant correlation (r = 0.87) indicates the existance of evaporites (Figure 7b). The correlation between Ca^{2+} and SO_4^{2-} is negative but weak (r = –0.176) (Figure 7a) implied

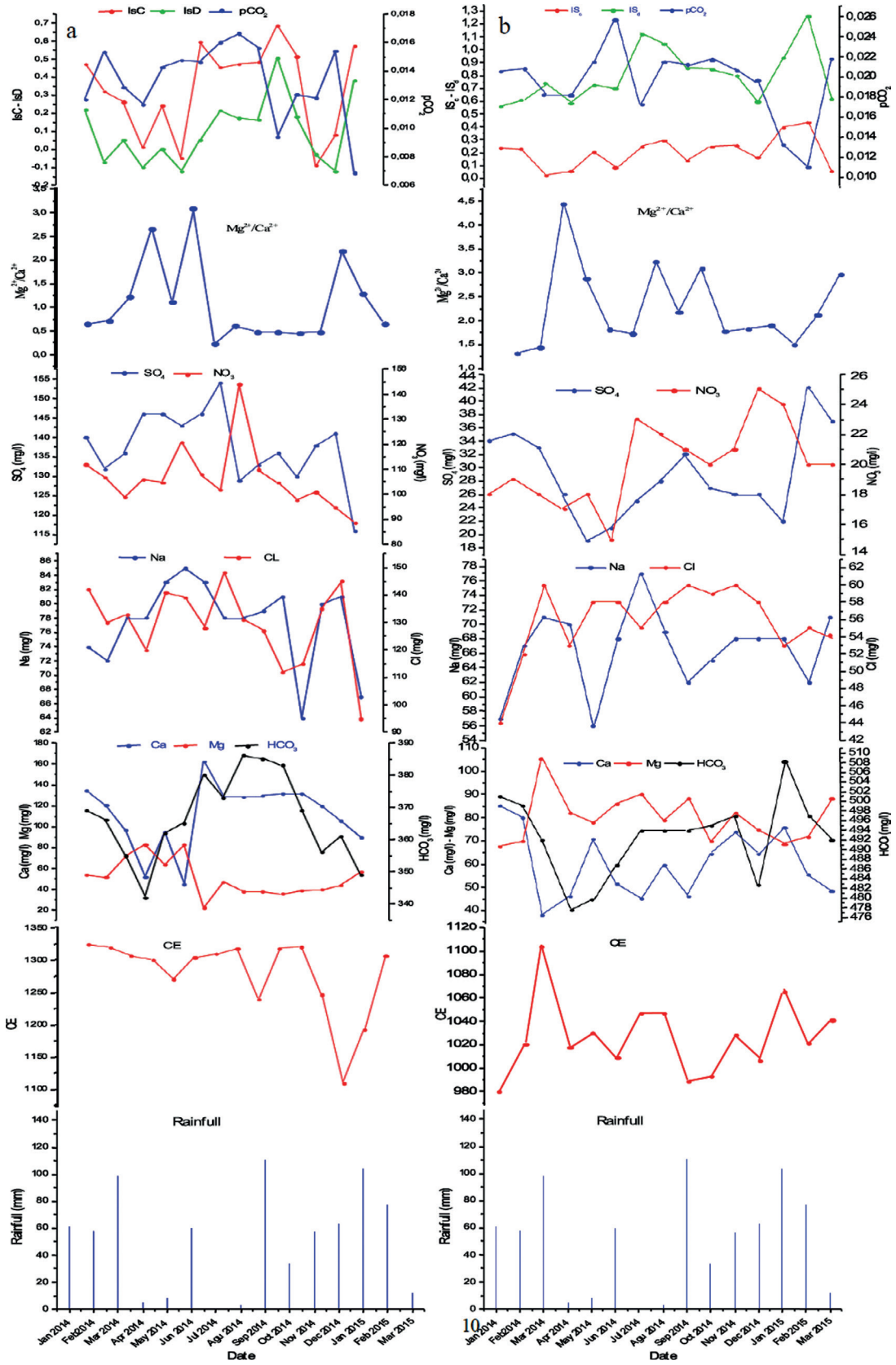

Figure 6. Temporal variations of precipitation, conductivity, chemical elements, ISc and ISd recorded in (a) the S6 spring (shallow water) and (b) the S1 spring (deep water).

Sigma J Eng Nat Sci, Vol. 40, No. 2, pp. 252–267, June, 2022

that Ca^{2+} was no derived from gypsum in the majority of samples, and indicates that the SO_4^{2-} is acquired in the unsaturated zone with direct infiltration. The carbonate rocks of the area rarely contain measurable concentrations of sulphur minerals. Thus, it can be concluded that agricultural-related parameters (nitrates and sulphates) are derived from fertilizers and manures applied on the agricultural areas [61]. In contrast, the water points whose chemistry is marked by gypsum or anhydrite have a good correlation between these elements (r = 0.93) (Figure 7b).

Shallow karst systems are easily contaminated by anthropogenic pollutants. Human effects are most evident in summer when recharge conveys high concentrations of nitrate from the farmed areas into the aquifer (Figure 6a). These

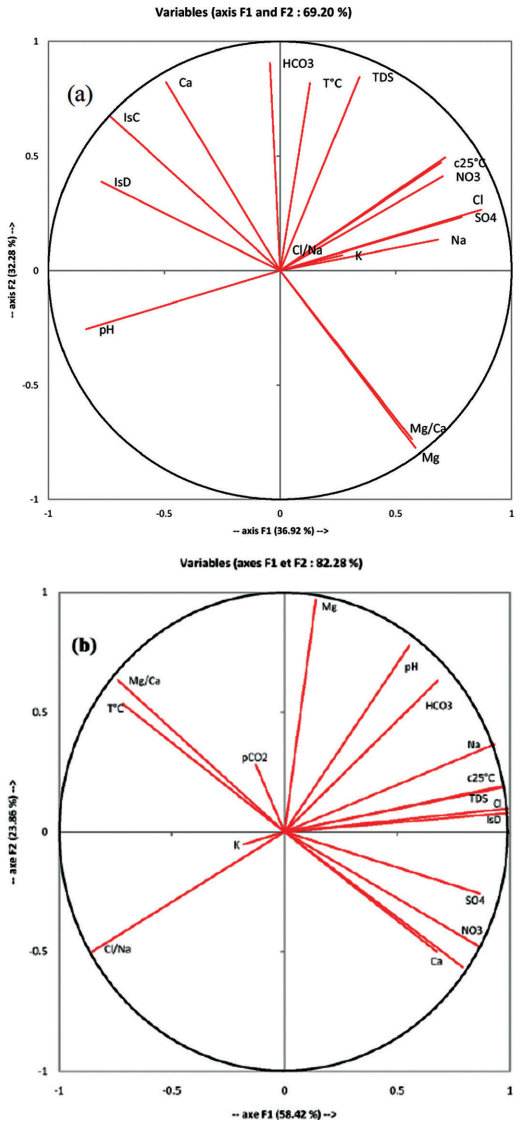

Figure 7. Distribution of the principal component analysis (PCA) scores: (a) all the aquifer springs and (b) the S4 spring.

shallow waters are much more vulnerable to NO_3^- contamination than the deep water. The variations of nitrates in shallow water are remarkable (with an increase of about 13 mg/l compared to the observed average), especially after the rains which follow a dry period (Figure 6a). However, the nitrate contents are relatively stable for deep water (Figure 6b). Generally, in shallow waters the NO_3^- concentrations presented a similar distribution as SO_4^{2-} and there is a positive correlation (r = 0.71) between them (Figure7a), suggesting a common source (Figure 6a). Both ions (SO_4^{2-} and NO_3^-) can be introduced with the urea and ammonium-sulphate applied during fertilization of the croplands [62]. The high concentration rate is explained by anthropogenic factors affecting water quality include impacts from agriculture, use of fertilizers [63], manure and pesticides, animal husbandry activities, domestic wastewater (existence of settling basins and non-watertight septic tanks). The nitrate deposits will be washed out to the outlet. The intense evaporation also produces an increase in NO_3^- [22, 64].

Generally, pCO_2 varies between 1.2×10^{-2} and 3.5×10^{-2} atm which is high than that of the atmosphere (3.4×10^{-4}atm). During the high water period the pCO_2 values are relatively stable (2.3×10^{-2} to 2.2×10^{-2} and 1.2×10^{-2} to 1.4×10^{-2}) (Figure 6a and b). While during low-water periods these values show a relative fluctuation.

The relatively high pCO_2 values indicate an open system on CO_2. In general, the saturation indices vary from saturated to oversaturated. The increase in HCO_3^- concentration with decrease in Mg^{2+}/Ca^{2+} molar ratio (Figures 6a and b) could be due to the increase in pCO_2 values [65, 10] or could have been due to saturation and precipitation of calcite [66]. The pCO_2 values confirm the carbonate origin of the groundwater and indicate that the residence time of the water is relatively long [66].The dolomites saturation indices are higher than those of the calcite in the majority of waters, reflecting the predominance of the dolomites. The negative values of the saturation index at surface sources after each heavy rain mean that the flows are at the unsaturated zone where the role of the dissolving power of the calcite with respect to the dolomite is determining (Figure 6a). Water in contact with carbonate rocks approaches the saturation with respect to calcite much faster than with respect to dolomite, since dolomite dissolution kinetics is approximately two orders of magnitude slower than calcite [4, 67–69]. The springs located in the south-western area which drains the deep waters shows supersaturating throughout the year (Figure 6b). The relatively high pCO_2 at the borehole level indicates a continuous infiltration of surface water towards the saturated zone.

The synchronous variation of NO_3^- and pCO_2 indicates the origin of surface water. The waters of Sidi Kada Mountains show inverse variations in pCO_2 with respect to ISd and ISc and mineralization (Figures 6a and b). During the period of high water, the systems which drain the unsaturated zone show ISc values lower than those of ISd. This

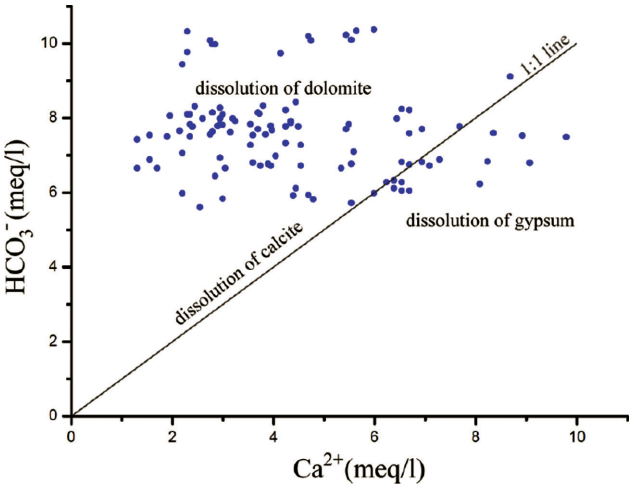

Figure 8. Diagram Ca^{2+} versus HCO_3.

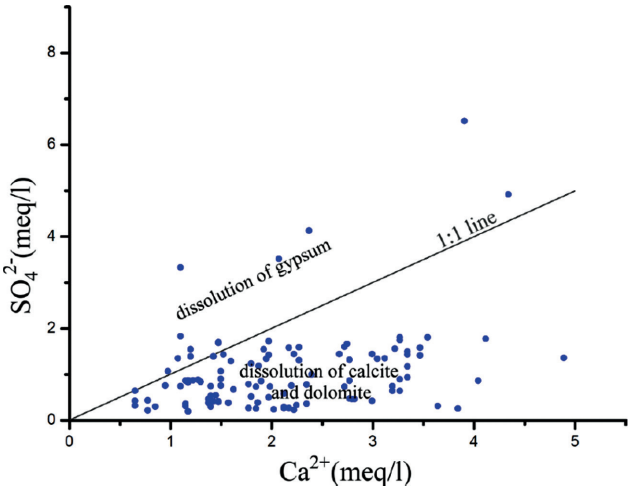

Figure 10. Diagram SO_4^{2-} versus Ca^2.

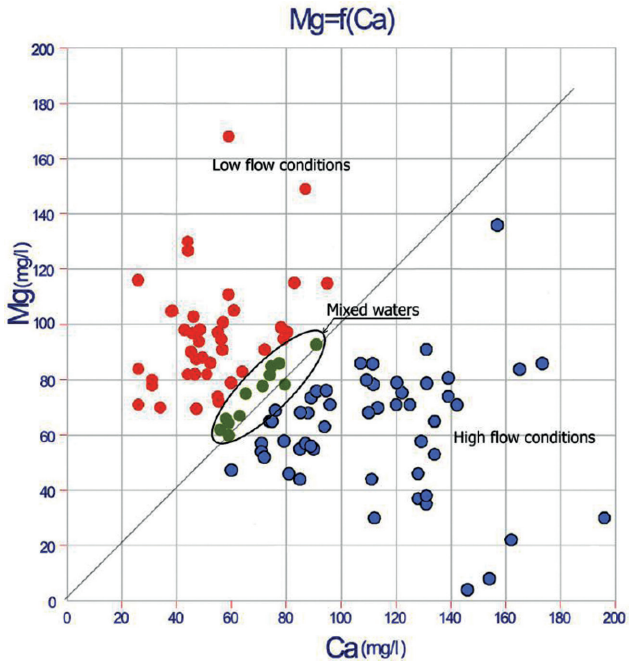

Figure 9. Diagram Mg^{2+} versus Ca^{2+}.

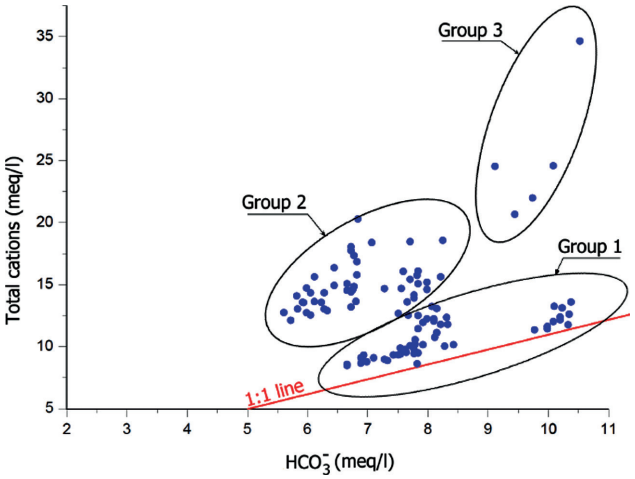

Figure 11. HCO_3^- versus total cations.

indicates the dissolution of calcite (Figure 6a). The variation of Sodium (Na^+) in the hydrogeological context of this system is related to climatic conditions. The origin of sodium, chlorides and sulphates in waters is from the soil surface. Leaching of these elements after evapotranspiration increases their concentrations by direct infiltration [70]. The chloride, sodium and sulphate ions are considered as surface markers [31, 27]. These hypotheses are confirmed by the significant agreements between Na^+ and SO_4^- (r = 0.85) and Na^+ and Cl^- (r = 0.75) (Figure 7a). Also, there are significant correlation between TDS and Mg^{2+} (r = 0.56), TDS and Na^+ (r = 0.61), TDS and Ca^{2+} (r = 0.53), TDS and Cl^- (r = 0.65), TDS and SO_4^{2-} (r = 0.77) and TDS and NO_3^- (r = 0.51) (Figures 7a and b), suggesting the influence of human activities on the water chemistry [62]. Exceptionally, the increased Na^+, Cl^- and SO_4^{2-} contents observed in group 3 (Table 1) could be attributed to the presence of the evaporites [71].

The evolution of HCO_3^- and Ca^{2+} contents shows synchronous fluctuations with high bicarbonate contents. Figure 8 illustrates that most of the water samples are plotted above the 1:1 line, showing that the HCO_3^- is greater than Ca^{2+}, which indicates the dissolution of dolomite. However, a part of water samples lie along the 1:1 line, suggesting that the main source of Ca^{2+} and HCO_3^- results from the dissolution of calcite. Furthermore, some water samples are under the 1:1 line, indicating that there is an excess of Ca^{2+}, which results from the dissolution of gypsum (Figure 8) [21, 72].

Sigma J Eng Nat Sci, Vol. 40, No. 2, pp. 252–267, June, 2022

These two elements (Ca^{2+} and HCO_3^-) are significantly correlated (r = 0.70) (Figure 7a).

The emergent waters that drain the south-western system of Sidi Kada Mountains throughout the year are characterized by Mg^{2+}/Ca^{2+} ratio more than 1 (Figure 6b). This may be due to the dissolution of Mg^{2+}, contained in the Kimmeridgien dolomites [73]. The other systems show Mg^{2+}/Ca^{2+} ratios less than 1 after the heavy rains which indicate that the waters are drained from the unsaturated zone with an average residence time of about 15 days. The diagram Ca^{2+} versus Mg^{2+} (Figure 9) shows the types of water according to their residence time: the waters above the 1:1 line indicate a long period of time (low flow conditions) [47] (Figure 9), while those below the 1:1 line indicate a short residence time (high flow conditions) and a predominance of water from the unsaturated zone. However, a part of water samples lie along the 1:1 line, suggesting a mixed waters.

Figure 10 shows the relation between Ca^{2+} and SO_4^{2-}. It is observed that some of the groundwater samples lie along the 1:1 line, suggesting that the dissolution of gypsum is a source for Ca^{2+} and SO_4^{2-}. Nevertheless, the Ca^{2+} and SO_4^{2-} concentrations in groundwater samples located above the 1:1 line result from simple gypsum dissolution because there are competing reactions involving calcium and/or sulphate ions. Indeed, a part from gypsum dissolution, cation concentrations may also be affected by ion exchange [74], which is justified by even the presence of clay in the aquifer formation. In the other hand, the most of groundwater samples lies below the 1:1 line, implying that dissolution of calcite and dolomite is dominant in this study area (Figure 10).

The relationship between HCO_3^- and the total cations illustrated in Figure 11 shows that the dissolution of carbonate increase alkalinity and total major cations with nearly a 1:1(group 1) [72]. The group 2 presents shallow water affected by the surface and the group 3 present the waters having an excess of SO_4^{2-} and Cl^- (Figure 11), that could be attributed to gypsum or anhydrite dissolution.

The waters of Sidi Kada Mountains are classified into three groups according to their degree of karstification and the residence time of the waters: a) Group 1, where ISc and ISd are generally greater than zero. This indicates non-aggressive waters with relatively slow circulation and corresponds to the drainage of water during low water periods (Figure 12); b) Group 2, where the waters are characterized by positive saturation indices with respect to calcite and negative with respect to dolomite. These indices indicate an average residence time (water arriving at the outlet about 45 days after a rainfall event). These waters are generally drained by piston effect during periods following floods (Figure 12); c) Group 3, which are characterized by negative saturation indices with respect to calcite and dolomite. This indicates aggressive waters with relatively rapid circulation. These waters which emerge following strong floods

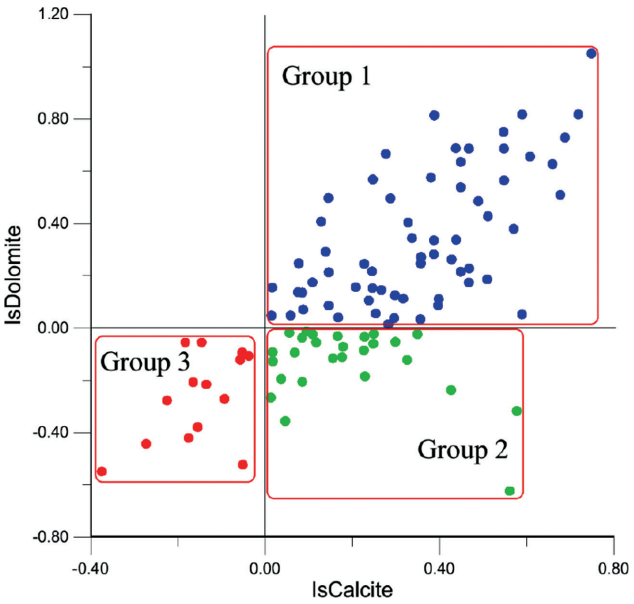

Figure 12. ISd/ISc diagram.

usually have a short residence time (water arriving at the outlet about 15 days after a rainfall event) (Figure 12). With the exception of shallow water during floods where the values are negative, the majority of the waters (about 87%) in the region generally have positive saturation indices with respect to calcite and dolomite (Figure 12).

CONCLUSION

Integrated analysis of hydrogeochemical data (EC frequency distribution, the time series of hydrochemical parameters) allow us to characterize the hydrogeological functioning of the karst aquifer in the Sidi Kada Mountains under variable hydroclimatic conditions. Magnesium–bicarbonate hydrochemical facies are usually indicative of dolomite as predominant mineral species in the aquifer. The frequency distributions of electrical conductivity (with its different peaks) is a useful tool for the identification of different sources of water and for studying the influence of hydrologic (recharge, recession and depletion) and climate conditions on the springs flow. The hydrogeological functioning of shallow water is much more influenced by the unsaturated zone than by the saturated zone (especially under recharge conditions). Both zones (saturated and unsaturated zone) present a relatively low degree of functional karstification. According to our results, the drained water characterizes the contribution of capacitive elements (small karst conduits, fractures and joints) to the groundwater flow, mainly in the saturated zone of the aquifer in the deep water.

The evolution of the analyzed physical and chemical parameters in response to rainfall events (high water

period) is characterized by marked decreases in EC of most parameters (Mg^{2+}, SO_4^{2-} and Cl^-), and an increase in Ca^{2+}.The waters drained are undersaturated or in equilibrium with respect to calcite, and presents relatively high values of pCO2, indicating a participation of the unsaturated zone; while the waters showing supersaturation indices indicate the participation of these waters in the saturated zone. The Mg^{2+} concentrations in the spring waters indicate different groundwater flow paths, with dissimilar lengths and residence times in the aquifer, but also a major proportion of dolomite. A good correlation between the sulphates, chlorides and nitrates is explained by anthropogenic impact. However, the good correlation between Ca^{2+} and SO_4^{2-} reflect the existence of gypsum lenses in our karst system.

The NO_3^- contents are high during floods and then gradually decrease. However, during the low water period, the drained water is more mineralized. The shallow karst zones accelerate the transport of recharge, so shallow systems respond quickly to rain events, always exhibiting rapid increases in EC. The Mg^{2+}/Ca^{2+} ratio indicates the predominance of dolomites in the study site. The high pCO_2 values, pH around 7 and the zero concentration of CO_3^{2-} ions indicate that the waters are drained in an opened system. The saturation indices for calcite and dolomite show that 87% of the water in the region is supersaturated. The waters in our system are less aggressive with relatively low flow velocity through a relatively small network of cracks.

In perspective, we suggest that a periodic monitoring should be performed with adequate sampling frequency in order to study and characterise the processes in which the aquifer is subject to various hydrodynamic conditions, because a better hydrogeological characterization is crucial for the protection and optimal management of these scarce water resources.

ACKNOWLEDGMENTS

The authors acknowledge Dr. Kacim Safir from the University of Mascara for the translation support. The author's thanks are also addressed to the national meteorology office (ONM) in Mascara (Algeria), the water resources national agency (ANRH) in Oran and the ADE in Mascara for having made available some field measurements.

AUTHORSHIP CONTRIBUTIONS

Authors equally contributed to this work.

DATA AVAILABILITY STATEMENT

The authors confirm that the data that supports the findings of this study are available within the article. Raw data that support the finding of this study are available from the corresponding author, upon reasonable request.

CONFLICT OF INTEREST

The author declared no potential conflicts of interest with respect to the research, authorship, and/or publication of this article.

ETHICS

There are no ethical issues with the publication of this manuscript.

REFERENCES

[1] Chalikakis K, Plagnes V, Guerin R, Valois R, Bosch FP. Contribution of geophysical methods to karst-system exploration: An overview. Hydrogeol J 2011;19:1169–1180. [CrossRef]

[2] White, W.B. 1988 Geomorphology and Hydrology of Karst Terrains. New York : Oxford University Press, 1988.

[3] Bakalowicz M. Karst groundwater: A challenge for new resources. Hydrogeol J 2005;13:148–160. [CrossRef]

[4] Ford D, Williams PD, Karst Hydrogeology and Geomorphology. Chichester, UK : John Wiley & Sons, 2007. [CrossRef]

[5] Goeppert N, Goldscheider N, Scholz H. Karst geomorphology of carbonatic conglomerates in the Folded Molasse zone of the Northern Alps (Austria/Germany). Geomorphology 2011;130:289–298. [CrossRef]

[6] Skoglund RØ, Lauritzen SE. Subglacial maze origin in low-dip marble stripe karst: examples from Norway. J Cave Karst Stud 2011;73:31–43. [CrossRef]

[7] Gil-Màrquez JM, Andreo B, Mudarra M. Combining hydrodynamics, hydrochemistry, and environmental isotopes to understand the hydrogeological functioning of evaporite-karst springs. J Hydrol 2019;576:299–314. [CrossRef]

[8] Stevanovic Z. (Ed.). Karst Aquifers - Characterization and Engineering, Professional Practice in Earth Sciences. Amsterdam: Springer International Publishing, 2015.

[9] Stevanovi´c Z. 2019. Karst waters in potable water supply: A global scale overview. Environ Earth Sci 2019;78:662. [CrossRef]

[10] Lorette G, Viennet D, Labat D, Massei N, Fournier M, Sebilo M, et al. Mixing processes of autogenic and allogenic waters in a large karst aquifer on the edge of a sedimentary basin (Causses du Quercy, France). J Hydrol 2021;593:125859. [CrossRef]

[11] Benrabah S, Attoui B, Hannouche M. Characterization of groundwater quality destined for drinking water supply of Khenchela City (eastern Algeria). J Water Land Dev 2016;30:13–20. [CrossRef]

[12] McGinley PM, Masarik KC, Gotkowitz MB, Mechenich DJ. Impact of anthropogenic geochemical change and aquifer geology on groundwater phosphorus concentrations. Appl Geochem 2016;72:1–9. [CrossRef]
[13] Kumar P, Thakur PK, Bansod BK, Debnath SK. Multi-criteria evaluation of hydro-geological and anthropogenic parameters for the groundwater vulnerability assessment. Environ Monit Assess 2017;189:564. [CrossRef]
[14] Masindi K, Abiye T. Assessment of natural and anthropogenic influences on regional groundwater chemistry in a highly industrialized and urbanized region: a case study of the Vaal River Basin, South Africa. Environ Earth Sci 2018;77:1–14. [CrossRef]
[15] Saba N, Umar R, Absar A. Estimation of anthropogenic influences in groundwater quality of shallow aquifers of Moradabad City, Western Uttar Pradesh. J Geol Soc India 2018;91:711–716. [CrossRef]
[16] Maas B, Peterson E, Honings J, Oberhelman A, Oware P, Rusthoven I, et al. Differentiation of surface water and groundwater in a Karst system using anthropogenic signatures. Geosciences 2019;9:148. [CrossRef]
[17] Patel MP, Gami B, Patel A, Patel P, Patel B. Climatic and anthropogenic impact on groundwater qual-ity of agriculture dominated areas of southern and central Gujarat, India. Groundw Sustain Dev 2020;10:1–11. [CrossRef]
[18] Thilagavathi R, Thivya C, Banajarani Panda (2020) Determination of the major geochemical processes of groundwater along the Cretaceous-Tertiary boundary of Trichinopoly, Tamilnadu, India. Acta Geochim 2020;39:760–781. [CrossRef]
[19] Khorrami B. Monitoring the spatio-temporal rends of groundwater qualitative parameters through geostatistical tools. Sigma J Eng Nat Sci 2019;37:1463–1475
[20] Huang H, Chen ZH, Wang T, Xiang CJ, Zhang L, Zhou GM, Sun BT, Wang Y. Nitrate distribution and dynamics as indicators to characterize karst groundwater flow in a mined mineral deposit in southwestern China. Hydrogeol J 2019;27:2077–2089. [CrossRef]
[21] Yongli G, Cheng Z, Qiong X, Hua B. Hydrogeochemical characteristics of a closed karst groundwater basin in North China. J Radioanal Nucl Chem 2020;325:365–379. [CrossRef]
[22] Tamburini A, Menichetti M. groundwater circulation in fractured and karstic aquifers of the umbria-marche apennine water. 2020;12:1039. [CrossRef]
[23] Zhang B, Zhao D , Zhou P, Qu S, Liao F, Wang G. Hydrochemical characteristics of groundwater and dominant water–rock interactions in the Delingha Area, Qaidam Basin, Northwest China Water 2020;12:836. [CrossRef]
[25] Mangin A. (Contribution à l'étude hydrodynamique des aquifères karstiques. Ann Spéléol 1975;30:21–124.
[26] Jeannin PY, Sauter M. Analysis of karst hydrodynamic behaviour using global approaches: a review. Bull Hydrogéol (Neuchâtel) 1998;16:31–48.
[27] De la Torre B, Mudarra M, Andreo B. Investigating karst aquifers in tectonically complex alpine areas coupling geological and hydrogeological methods. Hydrogeol J X 2020;6:100047. [CrossRef]
[28] Lastennet R, Mudry J. Role of karstification and rainfall in the behavior of a heterogeneous karst system. Environ Geol 1997;32(2):114–123. [CrossRef]
[29] Danquigny C, Emblanch C, Blondel T, Garry B, Roch A, Sudre C. Influence of great flood on the functioning of karst aquifer: Example of the Fontaine de Vaucluse karst system (SE France). In: Andreo B, Carrasco F, Duran JJ, LaMoreaux JW, editors. Berlin, Heidelberg: Springer, 2010:115–121. [CrossRef]
[30] Barbera J, Andreo B. Duality of functioning in a karst system under Mediterranean climate conditions, deduced from hydrochemical characterization. In: Andreo B, Carrasco F, Duran JJ, La Moreaux JW, editors. Advances in research in karst media. Berlin: Springer, 2010:189–194. [CrossRef]
[31] Bakalowicz M. Contribution de la géochimie des eaux à la connaissance de l'aquifère karstique et de la karstification [Contribution of water geochemistry to the knowledge of the karst aquifer and of the karstification]. Doctorat ès Sciences naturelles, P. et M. Curie Paris-6 University, Paris, 1979.
[32] Bakalowicz M. (La zone des infiltrations des aquifères karstiques. Méthode d'étude, structure et fonctionnement. Hydrogeologie 1995;4:3–21.
[33] Mudry J. Apport du traçage physico-chimique naturel à la connaissance hydrocinématique des aquifères carbonatés. Doctoral dissertation, Université de Franche-Comté, 1987.
[34] Moral F, Cruz-Sanjulian JJ, Olias M. Geochemical evolution of groundwater in the carbonate aquifers of Sierra de Segura (BeticCordillera, southern Spain). J Hydrol 2008;360:281–296. [CrossRef]
[35] Gastmans D, Chang HK, Hutcheon I. (2010) Groundwater geochemical evolution in the northern portion of the Guarani Aquifer System (Brazil) and its relationship to diagenetic features. Appl Geochem 2010;25:16–33. [CrossRef]
[36] Sánchez D, Barberá JA, Mudarra M, Andreo B. Hydrogeochemical tools applied to the study of carbonate aquifers: examples from some karst systems of Southern Spain. Environ Earth Sci 2015;74:199–215. [CrossRef]
[37] Massei N, Mahler B.J, Bakalowicz M, Fournier M, Dupont JP. Quantitative interpretation of

specific conductance frequency distributions in karst. Ground Water 2007;200:288–293. [CrossRef]
[38] Freeze RA, Cherry JA. Groundwater. New Jersey: Prentice Hall, 1979:604.
[39] Helsel DR, Hirsch RM. Graphical data analysis. Statistical methods in water resources. Virginia: Geological Survey, 2002:17–64.
[40] Şen Z. Groundwater quality. Practical and applied hydrogeology. Oxford: Elsevier, 2015:279–339. [CrossRef]
[41] Batiot C, Emblanch C, Blavous B. Carbone organique total (COT) et Magnésium (Mg2+): Deux traceurs complémentaires du temps de séjours dans l'aquifère karstique. CR Géosci 3003;335:205–214. [CrossRef]
[42] Barbera´ JA, Andreo B. Hydrogeological processes in a fluviokarstic area inferred from the analysis of natural hydrogeochemical tracers. The case study of eastern Serranı´a de Ronda (S Spain). J Hydrol 2015;523:500–514. [CrossRef]
[43] Mudarra M, and Andreo B. Hydrogeological functioning of a karst aquifer deduced from hydrochemical components and natural organic tracers present in spring waters. The case of Yedra Spring (Southern Spain). Acta Carsologica 2010;39:261–270. [CrossRef]
[44] Emblanch C, Blavoux B, Puig JM, Mudry J. Dissolved organic carbon of infiltration within the autogenic karst hydrosystem. Geophys Res Lett 1998;25:1459–1462. [CrossRef]
[45] Emblanch C, Zuppi GM, Mudry J, Blavoux B, Batiot C. Carbon 13 of TDIC to quantify the role of the unsaturated zone: the example of the Vaucluse karst system (Southeastern France). J Hydrol 2003;279:262–274. [CrossRef]
[46] Doctor DH, Alexander Jr, EC, Petric M, Kogovsek J, Urbanc J, Lojen S, et al. Quantification of karst aquifer discharge components through endmember mixing analysis using natural chemistry and isotopes as tracers. Hydrogeol J 2006;14:1171–1191. [CrossRef]
[47] Mudarra M, Andreo B. Relative importance of the saturated and the unsaturated zones in the hydrogeological functioning of karst aquifers: The case of Alta Cadena (Southern Spain). J Hydrol 2011;397:263–280. [CrossRef]
[48] Chrair M, Khaldi A, Hamadouche M, Hamimed A, Cernesson F, Alkan M. Evaluation of the effects of land cover changes and urbanization on land surface temperature: A remote sensing study of sub-watershed of oued fekan, northwest algeria. Sigma J Eng Nat Sci 2020;38:907–926.
[49] Chitresh S, Pankaj K, Rajarshi D, Ram A, Prashant B, Sustainability assessment of the groundwater quality in the Western India to achieve urban water security. Appl Water Sci 2019;9:73. [CrossRef]
[50] Smiler R. Diagram. Laboratory of Hydrogeology, Avignon University, France, 2005.
[51] Azzaz H, Cherchali M, Meddi M, Houha B, Puig JM, Achachi A. The use of environmental isotopic and hydrochemical tracers to characterize the functioning of karst systems in the Tlemcen Mountains, northwest Algeria.Hydrogeol J 2008;16:531–546. [CrossRef]
[52] Karimi H, Raeisi E, Bakalowicz M. Characterising the main karst aquifers of the Alvand basin, northwest of Zagros, Iran, by a hydrogeochemical approach. Hydrogeol J 2005;13:787–799. [CrossRef]
[53] Khayat S, Ghanem M, Tamimi A, Haddad M, Geyer S, Hötzl H, et al. Hydrochemistry and isotope hydrogeology in the Jericho area/Palestine. In The Water of the Jordan Valley. Berlin, Heidelberg: Springer, 2009: 325–348. [CrossRef]
[54] Leybourne ML, Betcher RN, Mcritchie WD, Kaszycki CA, Boyle DR. Geochemistry and stable isotopic composition of tufa waters and precipitates from the Interlake Region, Manitoba, Canada: Constraints on groundwater origin, calcitization, and tufa formation. Chem Geol 2009;260:221–233. [CrossRef]
[55] Perrin J, Jeannin PY and Cornaton F. The role of tributary mixing in chemical variations at a karst spring, Milandre, Switzerland. J Hydrol 2007;332:158–173. [CrossRef]
[56] Williams PW (2008) The role of the epikarst in karst and cave hydrogeology: a review. Int J Speleol 2008;37:1–10. [CrossRef]
[57] López-Chicano Bouamama M, Vallejos A, Pulido-Bosch A. Factors which determine the hydrochemical behaviour of karst spring. A case study of betic cordilleras, Spain. Appl Geochem 2001;16:1179–1192. [CrossRef]
[58] Hunkeler D, Mudry J. Hydrochemical methods. In: Goldscheider N, Drew D, editors. Methods in Karst Hydrogeology. London: Taylor and Francis, 2007:93–121.
[59] Pronk M, Goldscheider N, Zopfi J, Zwahlen F. Percolation and particle transport in the unsaturated zone of a karst aquifer. Groundwater 2009;47:361–369. [CrossRef]
[60] Lorette G, Lastennet R, Peyraube N, Deni A. Groundwater-flow characterization in multilayered karst aquifer on the edge of a sedimentary basin in western France. J Hydrol 2018;566:137–149. [CrossRef]
[61] Mudarra M, Andreo B, Barberá JA, Mudry J. Hydrochemical dynamics of TOC and NO3- contents as natural tracers of infiltration in karst aquifers. Environ Earth Sci 2014;71:507–523. [CrossRef]
[62] Dar FA, Perrin J, Ahmed S, Narayana AC, Riotte J. Hydrogeochemical characteristics of Karst Aquifer from a semi-arid region of Southern India

and impact of rainfall recharge on groundwater chemistry. Arab J Geoscience 2015;8:2739–2750. [CrossRef]

[63] Jalali M. Geochemistry characterization of groundwater in an agricultural area of Razan, Hamadan, Iran. Environ Geol 2009;56:1479–1488. [CrossRef]

[64] Henson WR, Huang L, Graham WD, Ogram A. Nitrate reduction mechanisms and rates in an unconfined eogenetic karst aquifer in two sites with different redox potential. Journal of GeophysicalResearch: Biogeosciences 2017;122:1062–1077. [CrossRef]

[65] Sadek M, El-Samie AS. Pollution vulnerability of the Quaternary aquifer near Cairo, Egypt, as indicated by isotopes and hydrochemistry. Hydrogeol J 2001;9:273–281. [CrossRef]

[66] Wang C, Xie Y, Liu S, McCallum J, Li Q, Wu J. Effects of diffuse groundwater discharge, internal metabolism and carbonate buffering on headwater stream CO2 evasion. Sci Total Environ 2021;777:146230. [CrossRef]

[67] Yehdegho B, Reichl P. Recharge areas and hydrochemistry of carbonate springs issuing from Semmering Massif, Austria, based on long-term oxygen-18 and hydrochemical data evidence. Hydrogeol J 2002;10:628–642. [CrossRef]

[68] White WB. Geomorphology and Hydrology of Karst Terrains. Oxford University Press: New York, USA, 1988.

[69] Appelo, C.A.J.; Postma, D. Geochemistry, Groundwater and Pollution, 2nd ed.; Balkema: Rotterdam, The Netherlands, 2005; ISBN 9780415364287. [CrossRef]

[70] Stroj A, Briški M, Oštrić M. Study of groundwater flow properties in a karst system by coupled analysis of diverse environmental tracers and discharge dynamics water. Water 2020;12:2442. [CrossRef]

[71] Barberá JA, Andreo B, Almeida C. Using non-conservative tracers to characterise karstification processes in the Merinos-Colorado-Carrasco carbonate aquifer system (southern Spain). Environ Earth Sci 2014;71:585–599. [CrossRef]

[72] Hoaghia MA, Moldovan A, Kovacs E, Mirea IC, Kenesz M, Brad T, et al. Water quality and hydrogeochemical characteristics of some karst water sources in Apuseni Mountains, Romania. Water 2021;13:857. [CrossRef]

[73] Devaraj N, Chidambaram S, Vasudevan U, Pradeep K, Nepolian M, Prasanna MV, et al. Determination of the major geochemical processes of groundwater along the Cretaceous-Tertiary boundary of Trichinopoly, Tamilnadu, India. Acta Geochim 2020;39:760–781. [CrossRef]

[74] Sappa G, FerrantiF, De Filippi F.M, Cardillo G. Mg2+ based method for the pertuso spring discharge evaluation. Water 2017;9:67. [CrossRef]

[75] Fidelibus MD, Gutiérrez F, Spilotro G. Human-induced hydrogeological changes and sinkholes in the coastal gypsum karst of Lesina Marina area (Foggia Province, Italy). Eng Geol 2011;118:1–19. [CrossRef]